0026-895X/08/7304-1141–1150
MOLECULAR PHARMACOLOGY
U.S. Government work not protected by U.S. copyright
Mol Pharmacol 73:1141–1150, 2008

Vol. 73, No. 4
43679/3322388
Printed in U.S.A.

Labeling of Dopamine Transporter Transmembrane Domain 1 with the Tropane Ligand *N*-[4-(4-Azido-3-[^{125}I]iodophenyl)butyl]-2β-carbomethoxy-3β-(4-chlorophenyl)tropane Implicates Proximity of Cocaine and Substrate Active Sites

M. Laura Parnas, Jon D. Gaffaney, Mu Fa Zou, John R. Lever, Amy Hauck Newman, and Roxanne A. Vaughan

Department of Biochemistry and Molecular Biology, University of North Dakota School of Medicine and Health Sciences, Grand Forks, North Dakota (M.L.P., J.D.G., R.A.V.); Medicinal Chemistry Section, National Institute on Drug Abuse, Intramural Research Program, Baltimore, Maryland (A.H.N., M-F.Z.); and Department of Radiopharmaceuticals, University of Missouri, Columbia, Missouri (J.R.L.)

ABSTRACT

The novel photoaffinity ligand *N*-[4-(4-azido-3-^{125}I-iodophenyl)-butyl]-2-β-carbomethoxy-3β-(4-chlorophenyl) tropane ([^{125}I]MFZ 2-24) was used to investigate the site for cocaine binding on the dopamine transporter (DAT). [^{125}I]MFZ 2-24 irreversibly labeled both rat striatal and expressed human DAT with high affinity and appropriate pharmacological specificity. Tryptic proteolysis of [^{125}I]MFZ 2-24 labeled DAT followed by epitope-specific immunoprecipitation demonstrated that the ligand becomes adducted almost exclusively to transmembrane domains (TMs) 1–2. Further localization of [^{125}I]MFZ 2-24 incorporation achieved by proteolyzing labeled wild-type and methionine mutant DATs with cyanogen bromide identified the sequence between residues 68 and 80 in TM1 as the ligand adduction site. This is in marked contrast to the previously identified attachment of the photoaffinity label [^{125}I]RTI 82 in TM6. Because [^{125}I]MFZ 2-24 and [^{125}I]RTI 82 possess identical tropane pharmacophores and differ only in the placement of the reactive azido moieties, their distinct incorporation profiles identify the regions of the protein adjacent to different aspects of the cocaine molecule. These findings thus strongly support the direct interaction of cocaine on DAT with TM1 and TM6, both of which have been implicated by mutagenesis and homology to a bacterial leucine transporter as active sites for substrates. These results directly establish the proximity of TMs 1 and 6 in DAT and suggest that the mechanism of transport inhibition by cocaine involves close interactions with multiple regions of the substrate permeation pathway.

Dopaminergic neurotransmission is regulated by dopamine transporters (DATs), which actively transport dopamine (DA) from the synapse back into the presynaptic cell. This activity is necessary for appropriate dopaminergic function (Giros et al., 1996), and DA imbalances associated with such psychiatric disorders as Parkinson's disease and attention deficit disorder have been hypothesized to result from transport dysregulation (Miller et al., 1999). DAT belongs to the SLC6 family of Na^+/Cl^- dependent symporters that couple downhill ion flux to uphill movement of substrate (Chen and Reith, 2000). DAT is closely related to the transporters for norepinephrine (NET) and serotonin (SERT), which are targets for many abused and therapeutic drugs, such as cocaine, methylphenidate, and fluoxetine. These and other drugs bind to these transporters and block re-uptake, resulting in elevated transmitter levels that lead to addiction or ameliorate neurological symptoms.

DAT contains twelve transmembrane (TM) domains, connected by intracellular (IL) and extracellular (EL) loops, with

This work was supported by DA15175 (R.A.V.), North Dakota Experimental Program to Stimulate Competitive Research (EPSCoR) Doctoral Dissertation Fellowship (M.L.P.), Ruth L. Kirschtein Predoctoral Fellowship F31–14857 (J.D.G), and the National Institute on Drug Abuse Intramural Research Program (A.H.N., M-F.Z.).

Article, publication date, and citation information can be found at http://molpharm.aspetjournals.org.

doi:10.1124/mol.107.043679.

ABBREVIATIONS: DAT, dopamine transporter; DA, dopamine; NET, norepinephrine; SERT, serotonin; TM, transmembrane; GBR 12909, 1-(2 (bis-(4-fluorophenyl)methoxy)ethyl)-4-(3-phenylpropyl)piperazine; dihydrochloride (vanoxerine); [^{125}I]RTI 82, 3β-(4-chlorophenyl)tropane-2β-carboxylic acid, 4-azido-3-[^{125}I]iodophenylester; [^{125}I]MFZ 2-24, *N*-[4-(4-azido-3-[^{125}I]iodophenyl)butyl]-2β-carbomethoxy-3β-(4-chlorophenyl)tropane; HEK, human embryonic kidney; CFT, 2β-carbomethoxy-3β-(4-fluorophenyl)tropane; Ab, antibody; KRH, Krebs-Ringer HEPES; PAGE, polyacrylamide gel electrophoresis; CNBr; cyanogen bromide; WT, wild type; IL, intracellular loop; EL, extracellular loop; h, human; r, rat; LeuT, *Aquifex aeolicus* leucine transporter.

N and C termini located in the cytoplasm. For inward transport, it is proposed that DA, Na^+ and Cl^- bind to an extracellularly facing conformation of DAT and are translocated through a permeation pathway via structural rearrangements of the TMs (Rudnick, 1998). Uptake blockers could interfere with this process by competing with substrates for binding or by preventing TM conformational changes. However, the details of the transport inhibition mechanism remain largely unknown, in part because the three-dimensional structure of DAT and identities of the substrate and blocker active sites remain poorly understood. Elucidation of the structural elements and conformational states involved in binding monoamine transport inhibitors thus remains an important objective.

The crystal structure of a bacterial Na^+-dependent leucine transporter, LeuT, has recently been determined (Yamashita et al., 2005). In LeuT, the leucine and Na^+ binding sites are found within a pocket created largely by TMs 1, 3, 6, and 8. TMs 1 and 6 are adjacent to each other and are separated into intracellular and extracellular halves (1a, 1b, 6a, and 6b) by central unwound regions that interact with leucine and Na^+. Many of the LeuT active site residues are conserved in DAT, and some have been shown to be essential for DA transport. Homology modeling suggests that DAT and LeuT possess significant structural and functional similarities (Indarte et al., 2007); however, LeuT is not inhibited by cocaine (Singh et al., 2007), and its structure has not revealed information pertinent to cocaine molecular mechanisms.

Our group has used irreversible photoaffinity analogs of cocaine and other DA uptake blockers to investigate the structure of the DAT inhibitor binding site. These compounds bind reversibly to DAT but contain a reactive azido (N_3) moiety that forms a covalent bond with adjacent polypeptide sequence. The incorporation sites of four irreversible analogs based on the structures of cocaine, GBR 12909, and benztropine have been mapped to regions containing TMs 1–2, TMs 4–7, or both (Vaughan, 1995; Vaughan and Kuhar, 1996; Vaughan et al., 1999, 2001), with more recent findings narrowing the incorporation site of 3β-(4-chlorophenyl)tropane-2β-carboxylic acid, 4-azido-3-^{125}I-iodophenylester ([^{125}I]RTI 82) to TM6 (Vaughan et al., 2007). Because labeling of the protein occurs at a site adjacent to the ligand-reactive group, the TM 1 and 2 and 4 to 7 regions of DAT identified in these studies could represent protein domains that contact different aspects of the ligands and contribute to different faces of shared or overlapping binding domains for multiple classes of uptake inhibitors.

In this report, we extend these findings by determining the adduction site on DAT for a novel cocaine-based photoaffinity ligand, *N*-[4-(4-azido-3-^{125}I-iodophenyl)butyl]-2β-carbomethoxy-3β-(4-chlorophenyl)tropane ([^{125}I]MFZ 2-24) (Zou et al., 2001; Lever et al., 2005). This compound contains a pharmacophore identical to [^{125}I]RTI 82 and differs only in the orientation of the phenylazido arm, which is appended from the tropane bridge nitrogen (Fig. 1A) rather than the tropane C2β ester moiety (Fig. 1B). Because both ligands contain the tropane ring, 2β-ester function, and 3β-phenyl ring structural elements (Fig. 1D) essential for cocaine binding (Carroll et al., 1992), they should be targeted to the same reversible binding site.

The results show that [^{125}I]MFZ 2-24 becomes adducted to the intracellular half of TM1 within a thirteen-amino acid sequence that contains residues crucial for DA binding and transport. This suggests that cocaine interacts with DAT very close to the TM1 DA and/or Na^+ binding sites, where it may compete with substrate or prevent conformational changes necessary for transport. Furthermore, the distinct incorporation profiles of [^{125}I]MFZ 2-24 and [^{125}I]RTI 82 provide direct evidence that DAT TMs 1 and 6 are in close three-dimensional proximity.

Materials and Methods

Materials. [^{125}I]MFZ 2-24 and [^{125}I]RTI 82 were synthesized and radioiodinated as described previously (Carroll et al., 1992; Lever et al., 1996; Zou et al., 2001; Lever et al., 2005). Human embryonic kidney (HEK) 293 cells were from American Type Culture Collection (Manassas, VA); electrophoresis reagents were from Bio-Rad Laboratories (Hercules, CA); cell culture reagents were from Mediatech (Herndon, VA); protease inhibitors and FuGENE transfection reagents were from Roche Applied Science (Indianapolis, IN); 2β-carbomethoxy-3β-(4-fluorophenyl)tropane ([^{3}H]CFT) was from PerkinElmer Life and Analytical Sciences (Waltham, MA); [^{3}H]DA and rainbow molecular mass markers were from GE Healthcare (Chalfont St. Giles, Buckinghamshire, UK); trypsin, trypsin inhibitor, dopamine, (−)-cocaine, GBR 12909, nomifensine, mazindol, de-

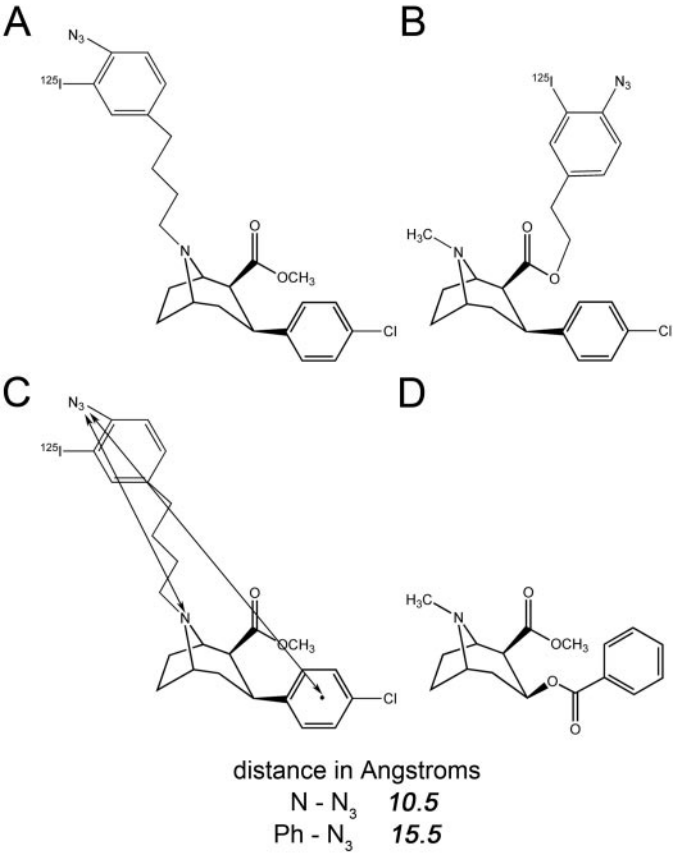

Fig. 1. Chemical structures of cocaine, [^{125}I]RTI 82, and [^{125}I]MFZ 2-24. A, [^{125}I]MFZ 2-24. The phenyl azido (N_3) moiety that undergoes covalent incorporation to the protein is appended to the tropane nitrogen. B, structure of [^{125}I]RTI 82 showing the phenyl azido moiety appended to the 2β ester moiety of the tropane ring. C, two-dimensional depiction of intramolecular distances in [^{125}I]MFZ 2-24, calculated using SYBYL 6.7 (Tripos, Inc., St. Louis, MO) and using the structure of CFT as a template. Energy minimization was performed by conjugate gradient method until a convergence gradient of 0.001 kcal/mol/Å was achieved. D, structure of cocaine.

sipramine, imipramine, and cyanogen bromide were from Sigma/RBI (Natick, MA); (+)-cocaine was the generous gift of Dr. Maarten Reith (New York University, New York, NY); the QuikChange mutagenesis kit was from Stratagene (La Jolla, CA); and synthetic oligonucleotide primers were purchased from Genscript Corp. (Piscataway, NJ) or MWG Biotech (High Point, NC). Male Sprague-Dawley rats were obtained from Charles River Laboratories, Inc. (Wilmington, MA) and were housed and treated in accordance with regulations approved by the University of North Dakota Institutional Animal Care and Use Committee.

Photoaffinity Labeling and in Situ Trypsin Proteolysis of Native DAT. Photoaffinity labeling of rat striatal membranes with [^{125}I]RTI 82 and [^{125}I]MFZ 2-24, in situ proteolysis, and DAT immunoprecipitation were performed essentially as described previously (Vaughan and Kuhar, 1996). For pharmacological studies, saturating concentrations (1–10 μM) of the nonradioactive transporter ligands were added to the binding mixture. For proteolysis studies, photolabeled rat striatal membrane suspensions were treated for 10 min at 22°C with equal volumes of trypsin prepared in sucrose phosphate buffer (10 mM Na_2PO_4 and 0.32 M sucrose, pH 7.4) using final trypsin concentrations of 10 to 200 μg/ml. At the end of the incubation, equal amounts of soybean trypsin inhibitor were added to halt digestion. Samples were centrifuged at 20,000*g* for 12 min at 4°C, and the resultant pellets were solubilized with 0.5% SDS sample buffer. Solubilized DATs or DAT fragments were subjected to epitope-specific immunoprecipitation as described previously (Vaughan and Kuhar, 1996; Vaughan et al., 1999) using antibody (Ab) 16 generated against rDAT N-terminal amino acids 42 to 59, or Ab 5 generated against rDAT EL2 amino acids 225 to 242. For peptide competition experiments, antisera were preabsorbed with 50 μg/ml peptide 16 or peptide 5 before sample addition. Total and immunoprecipitated samples were electrophoresed on 8 or 14% SDS-polyacrylamide gels followed by autoradiography using Hyperfilm MP or Kodak BioMax MS film for 1 to 4 days at −80°C. Low- and high-range rainbow markers were used as molecular mass standards.

Site-Directed Mutagenesis and Cell Culture. An N-terminal 6×His-human (h) DAT in a pcDNA3.1/HisB vector (kindly provided by Dr. J. B. Justice, Jr., Emory University, Atlanta, GA) was used as the starting template for mutagenesis of selected residues. hDAT mutants M111L/M116L, L80M/M111L/M116L, I67M/M111L/M116L, and M111L/M116L/M272L were generated using the QuikChange method (Stratagene). The entire DAT region was sequenced to verify mutations (Northwoods DNA, Solway, MN; Alpha BioLab, Burlingame, CA) and plasmids were introduced into HEK 293 cells (American Type Culture Collection) using FuGENE transfection reagent. Transformants were selected after 24 h by the addition of 600 μg/ml G418 (Geneticin) to the culture medium. Pooled stable cell lines were maintained at 37°C in complete medium (Dulbecco's modified Eagle's medium, 10% fetal bovine serum, 2 mM L-glutamine, 100 units/ml penicillin, and 100 μg/ml streptomycin) supplemented with 250 μg/ml G418 in an incubator gassed with 5% CO_2/95% O_2. Expression of mutants was verified by immunoblotting with hDAT-specific antibody (MAb 369; Millipore Bioscience Research Reagents, Temecula, CA) (Gaffaney and Vaughan, 2004). All mutants were assayed for cocaine-displaceable [^{3}H]DA uptake and binding of the cocaine analog 2β-carbomethoxy-3β-(4-fluorophenyl)tropane ([^{3}H]CFT) as described previously (Gaffaney and Vaughan, 2004; Vaughan et al., 2007).

Photoaffinity Labeling of Expressed DAT. Wild-type and mutant hDAT cells were plated onto six-well plates and grown to 90 to 95% confluence. Medium was removed, cells were washed twice with (KRH) buffer (25 mM HEPES, 125 mM NaCl, 4.8 mM KCl, 1.2 mM KH_2PO_4, 1.3 mM $CaCl_2$, 1.2 mM $MgSO_4$, and 5.6 mM glucose, pH 7.4). Reversible binding of ligand was accomplished by incubating cells with 5 nM [^{125}I]MFZ 2-24 prepared in KRH for 1 h at 22°C, followed by irreversible ligand incorporation into DAT by irradiation with 254 nm ultraviolet light for 45 s. Cells were washed twice with KRH and solubilized with Triton buffer (1% Triton X-100, 25 mM Tris base, 150 mM NaCl, and 1 mM EDTA) containing protease inhibitors on ice for 30 to 45 min with shaking. Lysates were centrifuged at 10,000*g* for 10 min at 4°C, and the supernatant was collected for analysis.

Electrophoresis and Autoradiography. Photoaffinity-labeled samples were subjected to SDS-PAGE and autoradiography on 10% acrylamide gels for intact DAT or 18 or 20% acrylamide gels for peptide fragments using high- and low-range Rainbow molecular mass markers as standards (Vaughan and Kuhar, 1996). For gel purification of DAT, the labeled band located at ~80 kDa was excised, and the protein was extracted by electroelution as described previously (Vaughan, 1995). Electroeluted samples were dialyzed for 18 h at 22°C against Milli Q water in a 10-kDa cut-off Slide-A-Lyzer dialysis cassette (Pierce, Rockford, IL) and evaporated to dryness in a SpeedVac concentrator (Thermo Fisher Scientific, Waltham, MA).

Cyanogen Bromide Digestion. Dried electroeluted DAT extracts were incubated for 24 h at 22°C in the dark in 0.1 ml of 70% formic acid with or without inclusion of 1 M cyanogen bromide (CNBr). Reactions were quenched with 0.9 ml of Milli Q water (Millipore, Billerica, MA) followed by drying in a SpeedVac concentrator, and the resulting pellets were subjected to three additional rounds of suspension in water and drying to remove volatile acidity. Dried samples were either prepared directly for electrophoresis by solubilization in 1× sample buffer or were resuspended in 50 mM Tris-HCl, pH 8.0, for immunoprecipitation.

Results

Irreversible Labeling of DAT with [^{125}I]MFZ 2-24. The development of [^{125}I]MFZ 2-24 as a ligand for biogenic amine transporters (Zou et al., 2001; Lever et al., 2005) and its irreversible incorporation into exogenously expressed hDAT and hSERT have been reported previously (Henry et al., 2006). [^{125}I]MFZ 2-24 labeling of native DATs in rat striatal membranes is shown in Figs. 2 to 4. [^{125}I]MFZ 2-24-labeled DAT was easily visible on SDS-PAGE gels at approximately 80 kDa in total membrane samples (not shown) and was the major labeled protein observed after immunoprecipitation (Figs. 2–4). Covalent labeling of DAT with [^{125}I]MFZ 2-24 was essentially completely inhibited when binding was carried out in the presence of DA or the DA uptake blockers (−)-cocaine, mazindol, GBR 12909, and nomifensine but was not significantly affected by (+)-cocaine or the NET and SERT inhibitors desipramine and imipramine (Fig. 2), supporting the pharmacological specificity of reversible binding and irreversible incorporation of this ligand.

Tryptic Mapping of the [^{125}I]MFZ 2-24 Labeling Site. Initial mapping of the [^{125}I]MFZ 2-24 DAT incorporation site was performed using trypsin, which cleaves at the C-terminal side of lysine and arginine residues, followed by epitope-specific immunoprecipitation of the fragments. Initial exper-

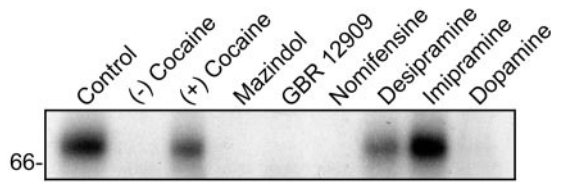

Fig. 2. Pharmacological profile of [^{125}I]MFZ 2-24 DAT labeling. Rat striatal membranes were photoaffinity-labeled with [^{125}I]MFZ 2-24 in the presence of the indicated compounds (10 μM final concentrations, except imipramine, which was 1 μM). Solubilized membranes were immunoprecipitated with DAT Ab16 and analyzed by SDS-PAGE and autoradiography. Molecular mass standards for all gels are indicated in kilodaltons.

iments were done in parallel with [^{125}I]RTI 82 labeled DAT to allow direct comparison of the incorporation profiles of the two ligands (Fig. 3A). Rat striatal membranes labeled with [^{125}I]MFZ 2-24 or [^{125}I]RTI 82 were treated with or without trypsin and subjected to immunoprecipitation with N-terminal Ab 16 or extracellular loop 2 (EL2) Ab 5 (Fig. 3A).

DATs labeled with [^{125}I]MFZ 2-24 produced a strongly labeled 45-kDa fragment that precipitated with Ab 16 (*arrow a*), and a very lightly labeled 32-kDa fragment that precipitated with Ab 5 and comigrated with an [^{125}I]RTI 82 labeled fragment (*arrow b*). A 45-kDa trypsin fragment precipitated by Ab 16 has been described previously from DATs labeled with GBR 12909 and benztropine photoaffinity ligands (Vaughan and Kuhar, 1996; Vaughan et al., 1999, 2005). This fragment is generated by cleavage of DAT at Arg^{218} (Fig. 3C) and consists of the N-terminal cytoplasmic tail, TMs 1 to 3, and the glycosylated region of EL2 (Vaughan and Kuhar, 1996). The generation of the same fragment from [^{125}I]MFZ 2-24 labeled DAT indicates that this ligand becomes incorporated in the same domain (Fig. 3C, shaded region). A small amount of this fragment generated by endogenous proteolysis in the absence of trypsin is seen in lane 1.

The 32-kDa fragment labeled with [^{125}I]RTI 82 that precipitates with Ab 5 (Fig. 3A, arrow b) has been previously characterized as containing most or all of the protein C-terminal to Arg^{218} including TMs 4 to 12 (Vaughan and Kuhar, 1996). The faint labeling of a similar fragment with [^{125}I]MFZ 2-24 indicates that a very small fraction of [^{125}I]MFZ 2-24 became attached in this domain. However, the vast majority of [^{125}I]MFZ 2-24 incorporation N-terminal to Arg^{218} demonstrated that the major sites of [^{125}I]MFZ 2-24 and [^{125}I]RTI 82 adduction occur in distinct regions of the DAT primary sequence. Dual labeling of these N- and C-terminal regions has also been found to greater or lesser extents for two GBR 12909 analogs (Vaughan and Kuhar, 1996; Vaughan et al., 2001) and is consistent with the interpretation that the ligands are positioned in the binding pocket in an orientation that permits access of the N_3 group to both of these sites.

Pharmacological Specificity of Fragments. To verify that the labeling of the [^{125}I]MFZ 2-24 fragments was pharmacologically specific, we incubated rat striatal DATs with [^{125}I]MFZ 2-24 in the presence or absence of 10 μM (−)-cocaine, followed by trypsin digestion and precipitation of fragments with Ab 16 (Fig. 3B). Full-length DAT (Fig. 3B, arrow a) as well as 45- and 14-kDa fragments (Fig. 3B, arrows b and c) were precipitated. The mass of the 14-kDa fragment and its retention of epitope 16 are consistent with cleavage at Arg^{125} or Lys^{133} in IL1 (Fig. 3C), which localizes the [^{125}I]MFZ 2-24 incorporation site to TMs 1 and 2 (Fig. 3C,

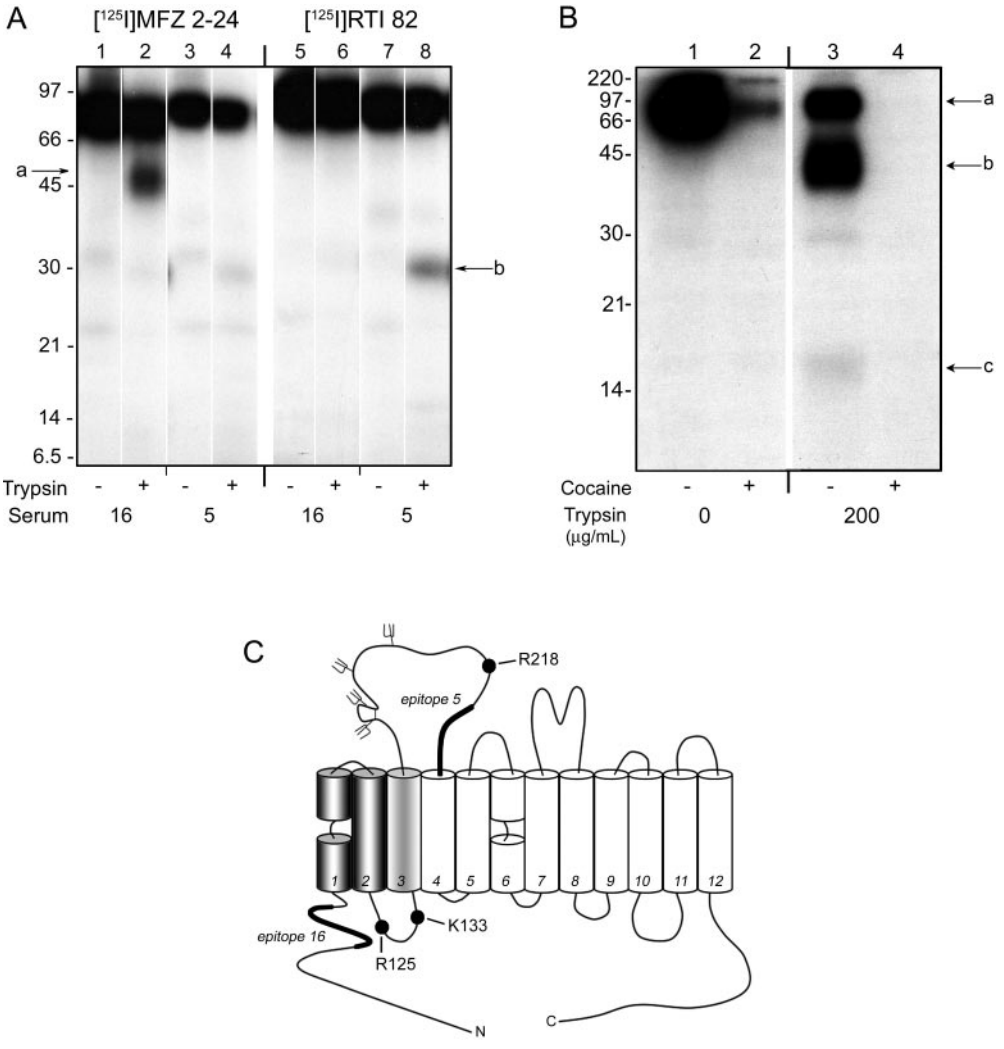

Fig. 3. [^{125}I]MFZ 2-24-labeled trypsin fragments. A, rat striatal membranes labeled with [^{125}I]MFZ 2-24 or [^{125}I]RTI 82 were treated with or without 50 μg/ml trypsin, and DAT and DAT fragments were immunoprecipitated with Ab16 or Ab 5 as indicated followed by SDS-PAGE and autoradiography. Samples were prepared and electrophoresed on the same gel exactly in parallel. Deletion of intervening lanes not included in final figure is indicated by white spaces and dividing lines. Arrow a, N-terminal 45-kDa fragment; arrow b, C-terminal 32-kDa fragment. B, rat striatal membranes were labeled with [^{125}I]MFZ 2-24 in the presence or absence of 10 μM (−)-cocaine, followed by treatment with or without 200 μg/ml trypsin, immunoprecipitation with Ab 16, and analysis by SDS-PAGE and autoradiography. *Arrow a*, full-length DAT protein; arrows b and c, 45- and 14-kDa labeled fragments. C, schematic diagram of rDAT showing the origin of the 45- and 14-kDa fragments in the primary sequence. TM domains are depicted as cylinders with TMs 1 and 6 shown with unwound central structure as described for LeuT, black circles show the positions of Arg^{125}, Lys^{133}, and Arg^{218} in IL1 and EL2 cleaved by trypsin to produce the 45- and 16-kDa N-terminal fragments, bold lines indicate epitopes for Abs 16 and 5, branches and line in EL2 indicate site of N-linked glycosylation and disulfide bond. Shading indicates TM domains present in 45-kDa fragment, light gray shading indicates the region cleaved from the 45-kDa fragment by proteolysis of IL1, and dark gray shading indicates TMs present in the 14-kDa fragment. White cylinders represent TMs present in 32-kDa Ab 5 precipitated fragment.

dark gray shading). Labeling of intact DAT and all fragments was essentially completely displaced by inclusion of cocaine (Fig. 3B, lanes 2 and 4), indicating that the fragments originated from the pharmacologically active binding site.

Immunological Specificity of Fragments. The immunological specificity of the [^{125}I]MFZ 2-24-labeled fragments is shown in Fig. 4. [^{125}I]MFZ 2-24-labeled striatal DATs treated without (Fig. 4, lanes 1 and 5) or with (Fig. 4, lanes 2–4 and 6–8) trypsin were immunoprecipitated with Ab 16 or Ab 5 preabsorbed with the indicated peptides. Precipitation of the 45 kDa photolabeled fragment with Ab 16 (Fig. 4, arrow a, lane 2) was significantly reduced by inclusion of peptide 16 (Fig. 4, lane 3) but not peptide 5 (Fig. 4, lane 4). Although the 14 kDa N-terminal fragment was not obtained here, in other experiments its precipitation with Ab 16 was blocked by peptide 16 but not by peptide 5 (not shown). Precipitation of the 32-kDa fragment by Ab 5 (Fig. 4, arrow b, lane 6) was prevented by inclusion of peptide 5 (Fig. 4, lane 7) but not peptide 16 (Fig. 4, lane 8). In this experiment, fragments of lower relative molecular mass fragments that were specifically immunoprecipitated by Ab 5 were also produced (Fig. 4, arrows c and d). The masses of these fragments, ~25 and 16 kDa, were similar to those obtained for [^{125}I]RTI 82-labeled DAT (Vaughan and Kuhar, 1996), consistent with the attachment of this small fraction of [^{125}I]MFZ 2-24 to TMs 4 to 7 and potentially to TM6. The band at ~32 kDa in the Ab 16-precipitated samples seems to be nonspecific, in that its precipitation is not effectively blocked by peptide 16, a finding that has been observed in previous studies (Vaughan et al., 2001).

CNBr Mapping of the [^{125}I]MFZ 2-24 Labeling Site. Because more precise localization of the [^{125}I]MFZ 2-24 incorporation site on DAT with trypsin is precluded by separation of labeled sites from Ab epitopes, we used a strategy involving chemical fragmentation of photolabeled DATs with CNBr, which specifically cleaves proteins on the C-terminal side of methionine residues. The human isoform of DAT possesses only 13 methionines throughout its sequence (Fig. 5). The N terminus through TMs 1 and 2 contains five methionines at positions 1 and 11 in the N-terminal tail and 106, 111, and 116 in TM2; the next methionines in the protein do not occur until positions 272 in TM5 and 371 at the top of TM7. For ease of discussion, we will refer to the CNBr fragments produced in this study by the flanking methionines, although the N-terminal residue in each fragment is actually the amino acid after the N-terminal cleavage site.

For CNBr analysis of DAT photolabeling sites, the starting samples consisted of [^{125}I]MFZ 2-24- or [^{125}I]RTI 82-labeled hDATs that were gel-purified and electroeluted. This removes other photolabeled proteins from the samples and solubilizes and denatures the protein so that all of the methionines are potentially available for proteolysis. In all CNBr experiments, control samples were treated with formic acid vehicle to verify that the fragments obtained were specific to CNBr cleavage and not produced by nonspecific acid hydrolysis. We also verified that all DATs analyzed in this study underwent CNBr cleavage by analyzing the 80-kDa forms on 8% SDS-PAGE gels (not shown). The CNBr-treated samples typically showed 50 to 80% losses of radioactivity, indicative of significant levels of proteolytic cleavage, although these losses are not easily seen in the high percentage gels and long film exposures required to visualize the fragments of low relative molecular mass.

CNBr mapping of [^{125}I]MFZ 2-24-labeled hDAT is shown in Fig. 6A. For this experiment, WT hDAT was labeled in the absence or presence of (−)-cocaine, treated with CNBr or vehicle, and immunoprecipitated with Ab 16. DATs treated with formic acid only migrated at ~80 kDa with no evidence for formation of fragments (lane 1), whereas CNBr treatment produced a prominently labeled fragment of ~12 kDa (lane 2, *arrow*) and a smaller amount of a slightly lower M_r form. Nonimmunoprecipitated samples show the same pattern (not shown), indicating that no other major CNBr fragments are produced. The masses of the labeled CNBr fragments are consistent with cleavage at one or more of the TM2 methionines, resulting in fragments that extend from Met^{1} or Met^{11} in the N-terminal tail through the methionine cluster

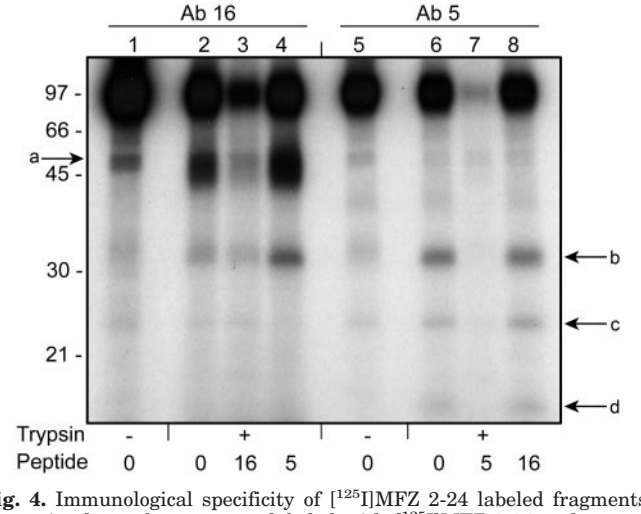

Fig. 4. Immunological specificity of [^{125}I]MFZ 2-24 labeled fragments. Rat striatal membranes were labeled with [^{125}I]MFZ 2-24 and treated with or without 100 μg/ml trypsin, followed by immunoprecipitation with Ab 16 or Ab 5 preabsorbed with 50 μg/ml peptide 16 or peptide 5 as indicated. Immunoprecipitated samples were analyzed by SDS-PAGE and autoradiography on a 16% gel. Arrow a, 45 kDa N-terminal fragment; arrows b, c, and d, 32-, 25-, and 16-kDa fragments precipitated by Ab 5.

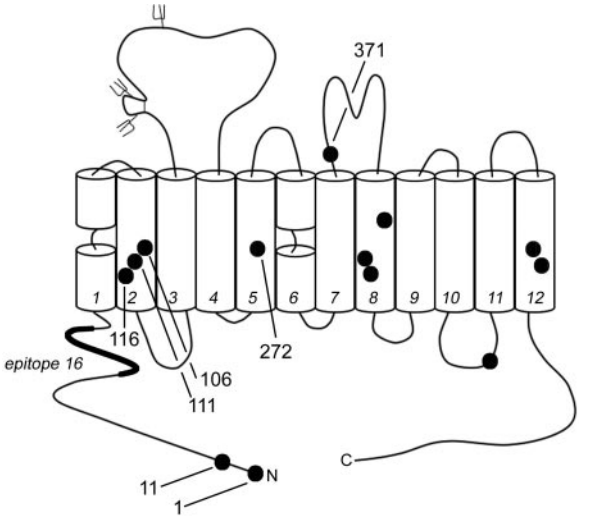

Fig. 5. Methionine residues in hDAT. Schematic diagram of hDAT showing positions of endogenous methionines. TM domains are depicted as cylinders with TMs 1 and 6 shown with unwound central regions, and endogenous methionines are shown as black circles with selected residues numbered. Branches and line in EL2 indicate site of N-linked glycosylation and disulfide bond, and bold line indicates epitope for Ab 16.

in TM2, and the Ab 16 precipitation of the fragments verifies their N-terminal origin. We do not know the basis for the production of the apparent doublet, but possibilities include incomplete proteolysis of Met^{11}, which would impart a mass difference of ~1 kDa between the fragments, nonspecific cleavage of unknown origin, or ubiquitylation or phosphorylation of N-terminal tail residues that may alter electrophoretic mobility (Foster et al., 2002; Miranda et al., 2007). DATs labeled in the presence of 10 μM (−)-cocaine show the absence of both the full-length protein (lane 3) and the CNBr fragments (lane 4), confirming the pharmacological origin of the fragments.

Although the masses of the fragments are consistent with cleavage of one or more of the TM2 methionines, we cannot determine from these data whether all of the methionines are cleaved. Thus, these results do not indicate whether the ligand attachment occurs N-terminal to Met^{106} or between the methionines in the cluster (Fig. 6A, shaded region of schematic diagram). To address this issue and more precisely delineate the site of [^{125}I]MFZ 2-24 adduction, we mutated endogenous methionines and inserted exogenous methionines in combinations that would generate CNBr fragments whose masses and immunoprecipitation characteristics would indicate the location of ligand attachment.

The hDAT constructs used for these studies were M111L/M116L, M111L/M116L/M272L, L80M/M111L/M116L, and I67M/M111L/M116L. All mutants were analyzed for expression, photoaffinity labeling, [^{3}H]DA transport, [^{3}H]CFT binding, and cocaine inhibition of [^{3}H]DA transport and [^{3}H]CFT binding. All mutants were expressed at levels comparable with the WT protein as analyzed by immunoblotting (not shown) and were active for cocaine-displaceable [^{125}I]MFZ 2-24 irreversible labeling (Figs. 6 and 7 and data not shown). All of the mutants displayed easily detectable [^{3}H]CFT binding and, except for L80M/M111L/M116L, which showed increased cocaine potency for transport inhibition, the IC_{50} values for cocaine inhibition of [^{3}H]DA transport and/or [^{3}H]CFT binding were not statistically different from the WT protein (Table 1), indicating that the mutations did not significantly affect the cocaine binding site. All of the mutants also possessed [^{3}H]DA transport activity that was comparable with that of the WT DAT except for L80M/M111L/M116L, which had reduced activity, and M111L/M116L/M272L, which was inactive (Table 1). The reduced transport activity of L80M/M111L/M116L hDAT compared with the WT protein and the M111L/M116L mutant is due not to lower total or surface expression but rather to a loss of Na^+ stimulation of transport (not shown), indicating the potential for Leu^{80} to function in the Na^+ dependence of transport. Work is currently underway in our laboratory to investigate the role of this residue more thoroughly (M. L. Parnas and R. A. Vaughan, manuscript in preparation).

To determine whether [^{125}I]MFZ 2-24 adduction occurs N-terminal to Met^{106}, we mutated both Met^{111} and Met^{116} to leucine to generate a protein (M111L/M116L) that contains only one methionine (Met^{106}) in TM2. The M111L/M116L hDATs were photolabeled in the presence or absence of 10 μM (−)-cocaine, followed by CNBr digestion and immunoprecipitation with Ab 16 (Fig. 6A). CNBr treatment of this mutant generates a 12-kDa fragment that precipitates with Ab 16 and is indistinguishable from that obtained from WT protein (Fig. 6A, lane 6, arrow). Labeling of the fragment is displaced by cocaine (Fig. 6A, lane 8), verifying its pharmacological specificity. These results demonstrate that Met^{106} is susceptible to CNBr cleavage and that [^{125}I]MFZ 2-24 adduction occurs N-terminal to this residue (Fig. 6A, shaded region in schematic diagram).

These results, however, do not eliminate the possibility

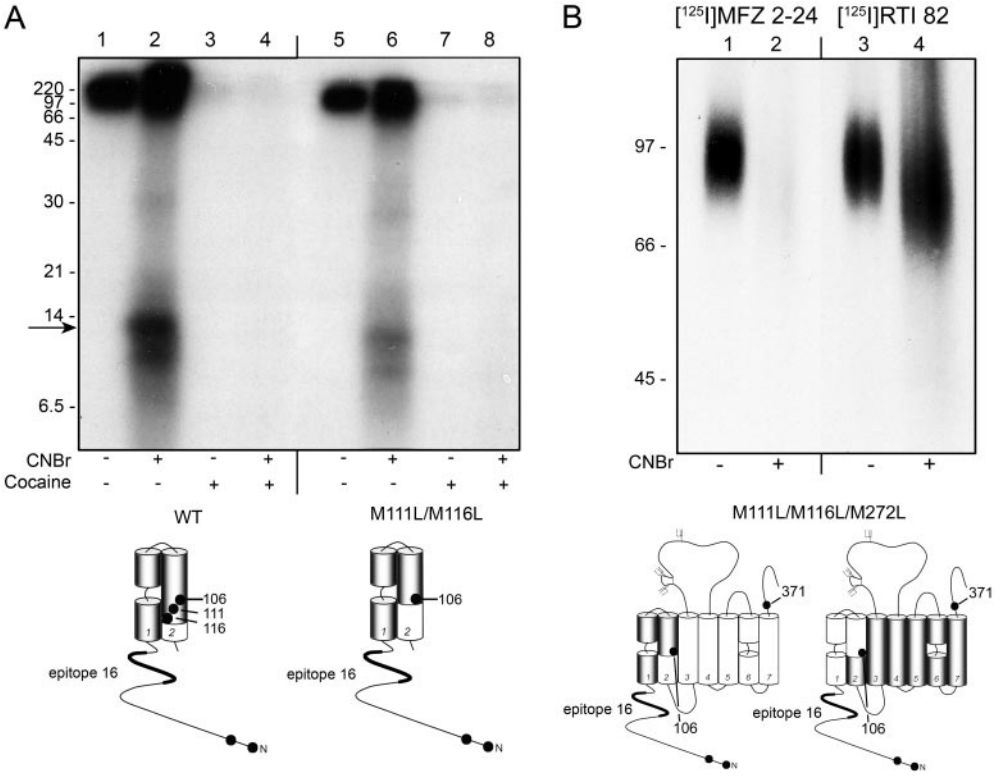

Fig. 6. CNBr digestion of [^{125}I]MFZ 2-24 labeled wild-type and methionine mutant hDATs. A. WT and M111L/M116L hDATs were labeled with [^{125}I]MFZ 2-24 in the presence or absence of 10 μM (−)-cocaine and treated with or without CNBr, followed by immunoprecipitation with Ab 16, and analysis by SDS-PAGE and autoradiography on an 18% gel. Arrow shows position of 12-kDa photoaffinity-labeled fragment, with *shading* in schematic diagram indicating protein region labeled. B, M111L/M116L/M272L hDATs were labeled with [^{125}I]MFZ 2-24 or [^{125}I]-RTI 82, treated with or without CNBr and analyzed by SDS-PAGE and autoradiography on an 8% gel. Schematic diagrams below both autoradiographs show the positions of the relevant methionine residues in each protein (black circles), and shading indicates the primary region labeled in each protein.

that [^{125}I]MFZ 2-24 also reacts between Met^{106} and Met^{116}. If this region were labeled and all of the methionines were cleaved, the resulting fragments would not be detected in either Fig. 6A or in total proteolyzed samples because they would not precipitate with Ab 16 and would be too small for analysis by SDS-PAGE. To address this issue, we mutated Met^{272} in TM5 to leucine in the M111L/M116L background to generate a protein (M111L/M116L/M272L) in which CNBr would produce a fragment extending from Met^{106} in TM2 to Met^{371} at the top of TM7 (Fig. 6B). This fragment would contain 265 amino acids (~30 kDa of protein) plus ~25 kDa of N-linked carbohydrates from EL2 for a total mass of ≥55 kDa, permitting analysis of the TM2 region C-terminal to Met^{106} by SDS-PAGE (Vaughan et al., 2007). Because [^{125}I]RTI 82 labels DAT in TM6, the removal of the TM5 CNBr site allows production of this fragment to be verified.

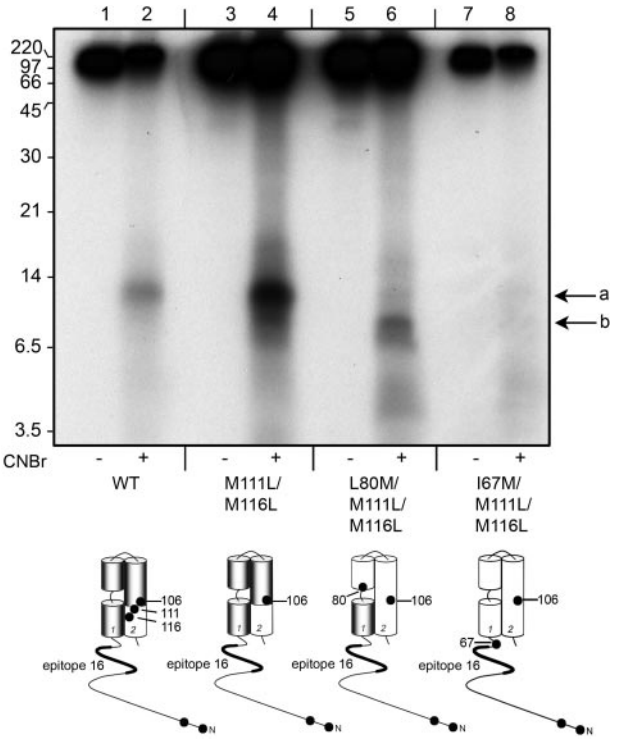

Fig. 7. Localization of [^{125}I]MFZ 2-24 adduction site in TM1. WT, M111L/M116L, L80M/M111L/M116L, and I67M/M111L/M116L hDATs were labeled with [^{125}I]MFZ 2-24, treated with or without CNBr, and subjected to immunoprecipitation with Ab 16, followed by SDS-PAGE and autoradiography on a 20% gel. Arrow a, fragment from WT and M111L/M116L hDATs; arrow b, fragment produced from L80M/M111L/M116L hDAT. The schematic diagrams below the autoradiograph show the positions of relevant endogenous and engineered methionines in each protein (black circles), and gray shading indicates regions consistent with the masses and immunoprecipitation characteristics of the fragments produced from each protein. The absence of labeled fragments in lane 8 indicates the separation of the photolabeled site from the Ab16 epitope via cleavage at I67M.

Figure 6B shows the analysis of the M111L/M116L/M272L hDAT construct labeled with [^{125}I]MFZ 2-24 (Fig. 6B, lanes 1 and 2) or [^{125}I]RTI 82 (lanes 3 and 4). CNBr digestion of the [^{125}I]RTI 82-labeled protein generated the predicted fragment visible at ~65 to 75 kDa (lane 4), whereas the [^{125}I]MFZ 2-24-labeled protein showed only an extremely minor amount of this fragment (lane 2), consistent with the fraction of label precipitated by Ab 5 in Figs. 3 and 4. This result conclusively localizes the region N-terminal to Met^{106} as the primary site of [^{125}I]MFZ 2-24 attachment. Note that in this experiment, the [^{125}I]MFZ 2-24-labeled N-terminal fragment was not retained on the gel because of the low acrylamide concentration needed to separate the large fragment from control unproteolyzed DAT.

Identification of [^{125}I]MFZ 2-24 Attachment Site in TM1. To further localize the site of [^{125}I]MFZ 2-24 adduction, we generated two additional hDAT constructs with methionine residues substituted at Leu^{80} and Ile^{67} in the M111L/M116L background. These mutants, L80M/M111L/M116L and I67M/M111L/M116L, were photoaffinity-labeled and subjected to CNBr digestion, immunoprecipitation with Ab 16, and SDS-PAGE/autoradiography in parallel with WT and M111L/M116L hDATs (Fig. 7).

CNBr digestion of WT and M111L/M116L hDATs generates the previously characterized 12-kDa fragment (Fig. 7, lanes 2 and 4, arrow a) that precipitates with Ab 16 and extends from Met^{1} or Met^{11} to Met^{106} (Fig. 7, shaded region of schematic diagram). The next construct, L80M/M111L/M116L possesses a CNBr cleavage site at position 80 in the middle of TM1. CNBr treatment of this protein produced a fragment of ~8 to 9 kDa that was precipitated by Ab 16 (lane 6, arrow b). The smaller mass of this fragment relative to that obtained from the WT protein is consistent with cleavage at L80M and the loss of 26 residues (~3 kDa), and its precipitation demonstrates that it retains epitope 16. These results strongly indicate that [^{125}I]MFZ 2-24 incorporation occurs N-terminal to L80M, because if adduction occurred C-terminal to this residue, the fragment produced would have a mass of only ~3 kDa and would not be precipitated because of the loss of the Ab 16 epitope. These experiments, however, do not exclude the possibility that some [^{125}I]MFZ 2-24 incorporation also occurs between L80M and Met^{106}.

The final mutant analyzed was I67M/M111L/M116L, in which a CNBr site was inserted at position 67 at the intracellular end of TM1 just C-terminal to the end of epitope 16 (Fig. 7). If incorporation of [^{125}I]MFZ 2-24 occurred N-terminal to I67M, CNBr proteolysis would generate a photolabeled

TABLE 1
Kinetic characteristics of hDAT methionine mutants
Data are presented as mean ± S.E.; n = 3.

hDAT form	[^{3}H]DA uptake	[^{3}H]CFT binding	Cocaine [^{3}H]DA Uptake	IC_{50} [^{3}H]CFT Binding
	pmol/min/mg	*pmol/mg*		*nM*
WT	236 ± 13	2.54 ± 0.63	867 ± 103	170 ± 39
M111L/M116L	405 ± 41*	3.71 ± 0.56	608 ± 76	123 ± 11
M111L/M116L/M272L	N.D.	1.08 ± 0.35	N.D.	106 ± 32
L80M/M111L/M116L	48 ± 3**	2.38 ± 0.69	145 ± 21*	104 ± 11
I67M/M111L/M116L	174 ± 13	2.53 ± 0.15	705 ± 147	129 ± 15

ND, non-detectable.
* $P < 0.01$, ** $P < 0.001$ relative to WT values (ANOVA).

fragment of ~7 kDa that would include epitope 16. Although a peptide of this mass would be easily detectable on these gels, no radiolabeled Ab 16-precipitated CNBr fragment was produced from this protein (Fig. 7, lane 8). This demonstrates that I67M was cleaved; otherwise, the 12-kDa fragment seen in lanes 2 and 4 would have been produced, and the lack of recovery of a labeled fragment strongly suggests that [^{125}I]MFZ 2-24 labels a site C-terminal to I67M that becomes separated from epitope 16 by proteolysis. In combination with the results obtained for the L80M/M111L/M116L protein, these findings indicate that [^{125}I]MFZ 2-24 adduction to DAT occurs in the 13-amino acid stretch between residues 68 and 80 in TM1.

Discussion

[^{125}I]MFZ 2-24 labeling of DAT between Asp^{68} and Leu^{80} strongly suggests that reversible cocaine binding occurs near this region. This domain corresponds to the unwound and TM1a regions of LeuT, motifs confirmed in DAT by homology modeling (Indarte et al., 2007), and several DAT residues near this sequence have been implicated as participating in substrate or uptake inhibitor actions. Asp^{79} in the unwound region (Fig. 8A, yellow circle) is necessary for both DA transport and cocaine binding (Kitayama et al., 1992), mutations of Phe^{69}, Leu^{80}, Phe^{86}, and Pro^{87} (Fig. 8A, tan circles) lead to loss of transport without significant effects on cocaine binding (Table 1; Lin et al., 1999; Lin et al., 2000), and mutations of Asp^{68} and Phe^{76} (Fig. 8A, blue circles) decrease cocaine affinity but improve DA affinity or K_m (Lin et al., 1999; Chen et al., 2001; Zhen et al., 2004). Many of these residues are conserved or homologous in NET and SERT, where they also function in transport inhibitor binding (Barker et al., 1998; Henry et al., 2003, 2006). In addition, mutation of Trp^{84} (Fig. 8A, red circle) interferes with conformational changes that reorient the protein from an outwardly to an inwardly facing form (Lin et al., 2000; Chen et al., 2004a,b), and the accompanying increase in cocaine affinity is consistent with kinetic predictions that cocaine binds an extracellularly facing transporter form (Chen and Justice, 1998; Chen et al., 2004a).

Substrate contact points in TM1 of LeuT occur at sites corresponding to DAT residues Ala^{77}, Leu^{80}, and Ala^{81} (Fig. 8A, circles with asterisks) and Na^+ ions are coordinated by residues corresponding to DAT Gly^{75}, Ala^{77}, Val^{78}, and Asn^{82} (Fig. 8A, circles with bold outlines). It has been postulated that Asp^{79} of DAT coordinates Na^+ (Yamashita et al., 2005) or interacts with the charged DA amine (Indarte et al., 2007), leading to its essential function in transport. Together, these findings strongly suggest that this region of DAT is part of the DA active site. Because all of these residues are within or immediately adjacent to the [^{125}I]MFZ 2-24 labeled sequence, our results suggest that cocaine binds to DAT at or near the TM1 DA binding site, where it may compete with DA for access, consistent with the known competitive mechanism of transport inhibition (Reith et al., 1992; Earles and Schenk, 1999).

In addition, in LeuT, substrate binding occurs in a pocket formed from the central regions of TMs 1, 3, 6, and 8 (Yamashita et al., 2005) (Fig. 8B). TMs 1 and 6 are adjacent to each other on one side of the active site such that residues in the unwound regions directly contact leucine and Na^+. Access of bound substrate to the cytoplasm is blocked by intracellular portions of TMs 1, 3, 6, and 8, and it is postulated that release of substrate from this site to the intracellular medium is achieved by movement of these regions, especially TMs 1a and 6b, which may possess significant flexibility because of the unwound structure (Yamashita et al., 2005). Binding of cocaine at this site thus presents the potential for inhibition of TM1a conformational changes needed to open the intracellular substrate path. Stabilization of TM1a as a mechanism of transport inhibition is also supported by the findings that the TM1a residues Asp^{68} and Phe^{76} of DAT and Tyr^{95} of SERT function in binding of multiple uptake inhibitors, including cocaine, GBR 12909, mazindol, and citalopram (Barker et al., 1998; Lin et al., 1999; Zhen et al., 2004; Henry et al., 2006).

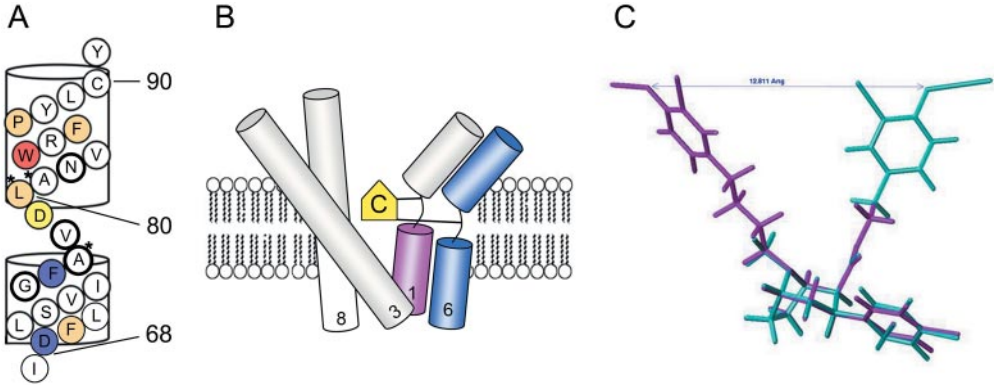

Fig. 8. Schematic representation of TM1 and potential cocaine binding pocket. A, helical net representation of DAT TM1 shown with presumed unwound region (Val^{78} and Asp^{79}), and inner and outer helices (*cylinders*). Adduction of [^{125}I]MFZ 2-24 occurs between residues Asp^{68} and Leu^{80}. Highlighted residues display the following properties upon mutation: tan, DA transport decreased; blue, cocaine affinity decreased; yellow, cocaine and DA affinity decreased; red, reduction of transport dependent conformational rearrangements. Circles with asterisks and bold outlines indicate homologous residues in LeuT that contact leucine or Na^+, respectively. B, schematic diagram of DAT active site based on structure of LeuT, showing formation of active site pocket by TMs 1, 3, 6, and 8. The yellow symbol (C) indicates cocaine bound in the substrate pocket such that the phenylazido moieties (lines) of [^{125}I]MFZ 2-24 or [^{125}I]RTI 82 extend to and form adducts within TM1 and TM6. Shading indicates the smallest region known to be labeled by [^{125}I]MFZ 2-24 (pink) and [^{125}I]RTI 82 (blue). C. Three-dimensional representation of [^{125}I]MFZ 2-24 (pink) and [^{125}I]RTI 82 (blue) showing superimposition of structure and relationship of phenylazido arm projections from pharmacophore. Intermolecular distance between [^{125}I]MFZ 2-24 and [^{125}I]RTI 82 azido groups was calculated using SYBYL 6.7 (Tripos, Inc.) and using the structure of CFT as a template. Energy minimization was performed by conjugate gradient method until a convergence gradient of 0.001 kcal/mol/Å was achieved.

Our results thus suggest that cocaine binds deep within the extracellularly facing crevice, where it competes with DA and/or locks TM1a in a conformation that prevents opening of the intracellular gate (Fig. 8B). These results contrast strongly with recent findings obtained by crystallization of LeuT bound to the tricyclic antidepressants desipramine and clomipramine (Singh et al., 2007; Zhou et al., 2007). In this case, the inhibitors were found to bind noncompetitively at a site extracellular to bound substrate, where they interacted with TM1 residues Arg^{30} and Gln^{34} (DAT Arg^{85} and Leu^{89}), resulting in stabilization of the extracellular gate. In addition, a noncompetitive binding site for ibogaine on the intracellular aspect of SERT has been deduced from sulfhydryl reagent reactivity (Jacobs et al., 2007), indicating that transport inhibition can occur via multiple molecular mechanisms.

The amino acid adduct for [^{125}I]MFZ 2-24 has not been identified, but because the azido group is not appended directly to the cocaine pharmacophore, adduction may occur at a residue near but not at a direct cocaine contact point. Molecular modeling of [^{125}I]MFZ 2-24 indicates distances of 10.5 and 15.5 Å between the azide and cocaine pharmacophore tropane N and 3β-phenyl ring (Fig. 1C). These could represent the distances between the N_3 adduction site and the pharmacophore structures, although it is important to note that the conformation of [^{125}I]MFZ 2-24 in the bound form is unknown, and the phenyl azido arm may be folded such that the distances between these pharmacophore moieties are less than the calculated estimates. Thus it is possible that [^{125}I]MFZ 2-24 reversible interaction with the protein could occur at a site that is somewhat more extracellular than the irreversibly labeled domain. However, with the exception of Trp^{84} (mutation of which affects cocaine affinity indirectly), the known TM1 mutations that affect cocaine affinity (Asp^{68}, Phe^{76}, and Asp^{79}) are in TM1a, consistent with reversible tropane interactions near this region.

Figure 8C shows a three-dimensional representation of the superimposed structures of [^{125}I]RTI 82 and [^{125}I]MFZ 2-24, highlighting the identity of the cocaine pharmacophores and the relative orientations of the phenylazido arms. The incorporation profiles of these ligands clearly suggest a binding orientation that places the tropane 2β ester moiety close to TM6 and the tropane bridge nitrogen close to TM1. This could position the positively charged tropane N near residues Ala^{77}, Val^{78}, and Asp^{79}, which have been modeled to interact with the positively charged DA amine (Indarte et al., 2007). The irreversible labeling of TMs 1 and 6 by [^{125}I]MFZ 2-24 and [^{125}I]RTI 82 also strongly suggests that these TMs are in close three-dimensional proximity, which to our knowledge is the first experimental evidence supporting this helix-packing arrangement in DAT. Although the attachment site for [^{125}I]RTI 82 within TM6 is not known, the adduction of [^{125}I]MFZ 2-24 to TM1a suggests the potential for [^{125}I]RTI 82 attachment to also occur near TM6b or the TM6 unwound region (Fig. 8B), which would place cocaine near another part of the substrate binding and permeation pathway. The minor amount of [^{125}I]MFZ 2-24 attachment to the TM 4 to 7 region may occur if the phenylazido arm folds with an orientation similar to that of [^{125}I]RTI 82, allowing reactivity with TM6. In contrast, we have never observed even minor amounts of [^{125}I]RTI 82 attachment in TMs 1 and 2, indicating that its shorter phenyl azido arm cannot extend to this region.

These ligand incorporation profiles also indicate that the bound compounds are oriented such that the plane of the molecule defined by the tropane ring nitrogen and 2β ester groups faces TMs 1 and 6, whereas the opposite side of the tropane ring and 3β phenyl ring may face other binding pocket domains. This is likely to include other nearby substrate sites, such as TM8 (Indarte et al., 2007) or TM3, which in SERT has been experimentally established to be adjacent to TM1 (Henry et al., 2006; White et al., 2006). Our group has not identified domains other than TMs 1 and 2 and 4 to 7 by irreversible inhibitor labeling, potentially because the N_3 groups of the compounds analyzed to date are not present in positions oriented toward other DAT sites. The recent development of a novel photoafffinity ligand for DAT that has its azido group appended to the 3β-aryl ring system (Newman et al., 2006) will aid in investigation of these possibilities.

Because irreversible GBR 12909 and benztropine compounds also attach to TMs 1–2 and 4–7, their binding sites may occur at or near the [^{125}I]MFZ 2-24 or [^{125}I]RTI 82 sites, although the extent of similarity is currently unknown. With respect to this issue, we found that for [^{125}I]MFZ 2-24-labeled DATs, production of the 14-kDa trypsin fragment generated by IL1 cleavage occurred with much lower stoichiometry than the same fragment from DATs labeled with the GBR 12909 ligand [^{125}I]1-[2-(diphenylmethoxy)-ethyl]-4-[2-(4-azido-3-iodophenyl)ethyl]piperazine (Wilson et al., 1989; Vaughan and Kuhar, 1996), suggesting that [^{125}I]MFZ 2-24 adduction to DAT induces a conformation that protects IL1 from proteolysis. Differential conformations of DAT IL1 induced by cocaine and benztropine binding have also been detected by reactivity of sulfhydryl reagents to Cys^{135} (Reith et al., 2001). We also previously found that DATs labeled with [^{125}I]RTI 82 or]^{125}I]1-[2-(diphenylmethoxy)ethyl]-4-[2-(4-azido-3-iodophenyl)ethyl]piperazine show differential protease sensitivities at Arg^{218} in EL2; again, the tropane labeled protein was more protease-resistant (Vaughan and Kuhar, 1996; Vaughan et al., 2001). These results suggest that cocaine and GBR 12909 analogs induce different conformations of DAT IL1 and EL2, which may differentially affect various transport functions or interactions with intracellular binding partners that ultimately lead to the differential behavioral endpoints observed for these classes of drugs (Rothman et al., 2008).

Acknowledgments

We thank Dr. Santosh Kulkarni (Medicinal Chemistry Section, NIDA-IRP) for the distance measurements in Figs. 1 and 8, Dr. Joseph B. Justice, Jr. (Emory University), for providing the WT 6xHis-hDAT construct, and Dr. James Foster (University of North Dakota) for valuable suggestions on construction of point mutants and assistance with artwork.

References

Barker EL, Perlman MA, Adkins EM, Houlihan WJ, Pristupa ZB, Niznik HB, and Blakely RD (1998) High affinity recognition of serotonin transporter antagonists defined by species-scanning mutagenesis. An aromatic residue in transmembrane domain I dictates species-selective recognition of citalopram and mazindol. *J Biol Chem* **273:**19459–19468.

Carroll FI, Gao Y, Abraham P, Lewin AH, Lew R, Patel A, Boja JW, and Kuhar MJ (1992) Probes for the cocaine receptor. Potentially irreversible ligands for the dopamine transporter. *J Med Chem* **35:**1813–1817.

Chen N and Justice JB Jr (1998) Cocaine acts as an apparent competitive inhibitor at the outward-facing conformation of the human norepinephrine transporter: kinetic analysis of inward and outward transport. *J Neurosci* **18:**10257–10268.

Chen N and Reith ME (2000) Structure and function of the dopamine transporter. *Eur J Pharmacol* **405:**329–339.

Chen N, Vaughan RA, and Reith ME (2001) The role of conserved tryptophan and acidic residues in the human dopamine transporter as characterized by site-directed mutagenesis. *J Neurochem* **77:**1116–1127.

Chen N, Zhen J, and Reith ME (2004a) Mutation of Trp84 and Asp313 of the dopamine transporter reveals similar mode of binding interaction for GBR12909 and benztropine as opposed to cocaine. *J Neurochem* **89:**853–864.
Chen NH, Reith ME, and Quick MW (2004b) Synaptic uptake and beyond: the sodium- and chloride-dependent neurotransmitter transporter family SLC6. *Pflugers Arch* **447:**519–531.
Earles C and Schenk JO (1999) Multisubtrate mechanism for the inward transport of dopamine by the human dopamine transporter expressed in HEK cells and its inhibition by cocaine. *Synapse* **33:**230–238.
Foster JD, Pananusorn B, and Vaughan RA (2002) Dopamine transporters are phosphorylated on N-terminal serines in rat striatum. *J Biol Chem* **277:**25178–25186.
Gaffaney JD and Vaughan RA (2004) Uptake inhibitors but not substrates induce protease resistance in extracellular loop two of the dopamine transporter. *Mol Pharmacol* **65:**692–701.
Giros B, Jaber M, Jones SR, Wightman RM, and Caron MG (1996) Hyperlocomotion and indifference to cocaine and amphetamine in mice lacking the dopamine transporter. *Nature* **379:**606–612.
Henry LK, Adkins EM, Han Q, and Blakely RD (2003) Serotonin and cocaine-sensitive inactivation of human serotonin transporters by methanethiosulfonates targeted to transmembrane domain I. *J Biol Chem* **278:**37052–37063.
Henry LK, Field JR, Adkins EM, Parnas ML, Vaughan RA, Zou MF, Newman AH, and Blakely RD (2006) Tyr-95 and Ile-172 in transmembrane segments 1 and 3 of human serotonin transporters interact to establish high affinity recognition of antidepressants. *J Biol Chem* **281:**2012–2023.
Indarte M, Madura JD, and Surratt CK (2007) Dopamine transporter comparative molecular modeling and binding site prediction using the LeuT(Aa) leucine transporter as a template. *Proteins* **10:**1033–1046.
Jacobs MT, Zhang YW, Campbell SD, and Rudnick G (2007) Ibogaine, a noncompetitive inhibitor of serotonin transport, acts by stabilizing the cytoplasmic-facing form of the transporter. *J Biol Chem* **282:**29441–29447.
Kitayama S, Shimada S, Xu H, Markham L, Donovan DM, and Uhl GR (1992) Dopamine transporter site-directed mutations differentially alter substrate transport and cocaine binding. *Proc Natl Acad Sci U S A* **89:**7782–7785.
Lever JR, Scheffel U, Stathis M, Seltzman HH, Wyrick CD, Abraham P, Parham K, Thomas BF, Boja JW, Kuhar MJ, et al. (1996) Synthesis and in vivo studies of a selective ligand for the dopamine transporter: 3 beta-(4-[125I]iodophenyl) tropan-2 beta-carboxylic acid isopropyl ester ([125I]RTI-121). *Nucl Med Biol* **23:**277–284.
Lever JR, Zou MF, Parnas ML, Duval RA, Wirtz SE, Justice JB, Vaughan RA, and Newman AH (2005) Radioiodinated Azide and isothiocyanate derivatives of cocaine for irreversible labeling of dopamine transporters: synthesis and covalent binding studies. *Bioconjug Chem* **16:**644–649.
Lin Z, Wang W, Kopajtic T, Revay RS, and Uhl GR (1999) Dopamine transporter: transmembrane phenylalanine mutations can selectively influence dopamine uptake and cocaine analog recognition. *Mol Pharmacol* **56:**434–447.
Lin Z, Wang W, and Uhl GR (2000) Dopamine transporter tryptophan mutants highlight candidate dopamine- and cocaine-selective domains. *Mol Pharmacol* **58:**1581–1592.
Miller GW, Gainetdinov RR, Levey AI, and Caron MG (1999) Dopamine transporters and neuronal injury. *Trends Pharmacol Sci* **20:**424–429.
Miranda M, Dionne KR, Sorkina T, and Sorkin A (2007) Three ubiquitin conjugation sites in the amino terminus of the dopamine transporter mediate protein kinase C-dependent endocytosis of the transporter. *Mol Biol Cell* **18:**313–323.
Newman AH, Cha JH, Cao J, Kopajtic T, Katz JL, Parnas ML, Vaughan R, and Lever JR (2006) Design and synthesis of a novel photoaffinity ligand for the dopamine and serotonin transporters based on 2beta-carbomethoxy-3beta-biphenyltropane. *J Med Chem* **49:**6621–6625.
Reith ME, de Costa B, Rice KC, and Jacobson AE (1992) Evidence for mutually exclusive binding of cocaine, BTCP, GBR 12935, and dopamine to the dopamine transporter. *Eur J Pharmacol* **227:**417–425.
Reith ME, Berfield JL, Wang LC, Ferrer JV, Javitch JA (2001) The uptake inhibitors cocaine and benztropine differentially alter the conformation of the human dopamine transporter. *J Biol Chem* **276:**29012–29018.
Rothman RB, Baumann MH, Prisinzano TE, and Newman AH (2008) Dopamine transport inhibitors based on GBR12909 and benztropine as potential medications to treat cocaine addiction. *Biochem Pharmacol* **75:**2–16.
Rudnick G (1998) Bioenergetics of neurotransmitter transport. *J Bioenerg Biomembr* **30:**173–185.
Singh SK, Yamashita A, and Gouaux E (2007) Antidepressant binding site in a bacterial homologue of neurotransmitter transporters. *Nature* **448:**952–956.
Vaughan RA (1995) Photoaffinity-labeled ligand binding domains on dopamine transporters identified by peptide mapping. *Mol Pharmacol* **47:**956–964.
Vaughan RA, Agoston GE, Lever JR, and Newman AH (1999) Differential binding of tropane-based photoaffinity ligands on the dopamine transporter. *J Neurosci* **19:**630–636.
Vaughan RA, Gaffaney JD, Lever JR, Reith ME, and Dutta AK (2001) Dual incorporation of photoaffinity ligands on dopamine transporters implicates proximity of labeled domains. *Mol Pharmacol* **59:**1157–1164.
Vaughan RA and Kuhar MJ (1996) Dopamine transporter ligand binding domains. Structural and functional properties revealed by limited proteolysis. *J Biol Chem* **271:**21672–21680.
Vaughan RA, Parnas ML, Gaffaney JD, Lowe MJ, Wirtz S, Pham A, Reed B, Dutta SM, Murray KK, and Justice JB (2005) Affinity labeling the dopamine transporter ligand binding site. *J Neurosci Methods* **143:**33–40.
Vaughan RA, Sakrikar DJ, Parnas ML, Adkins S, Foster JD, Zou MF, Duval R, Lever JR, Kulkarni SS, and Newman AH (2007) Incorporation of the cocaine analog [^{125}I]RTI 82 in transmembrane domain six of the dopamine transporter. *J Biol Chem* **282:**8915–8925.
White KJ, Kiser PD, Nichols DE, and Barker EL (2006) Engineered zinc-binding sites confirm proximity and orientation of transmembrane helices I and III in the human serotonin transporter. *Protein Sci* **15:**2411–2422.
Wilson AA, Grigoriadis DE, Dannals RF, Ravert HT, and Wagner HN Jr (1989) A one-pot radiosynthesis of [^{125}I]iodoazido photoaffinity labels. *J Labelled Comp Radiopharm* **27:**1299–1305.
Yamashita A, Singh SK, Kawate T, Jin Y, and Gouaux E (2005) Crystal structure of a bacterial homologue of Na^+/Cl^--dependent neurotransmitter transporters. *Nature* **437:**215–223.
Zhen J, Maiti S, Chen N, Dutta AK, and Reith ME (2004) Interaction between a hydroxypiperidine analogue of 4-(2-benzhydryloxy-ethyl)-1-(4-fluorobenzyl)piperidine and Aspartate 68 in the human dopamine transporter. *Eur J Pharmacol* **506:**17–26.
Zhou Z, Zhen J, Karpowich NK, Goetz RM, Law CJ, Reith ME, and Wang DN (2007) LeuT-desipramine structure reveals how antidepressants block neurotransmitter reuptake. *Science* **317:**1390–1393.
Zou MF, Kopajtic T, Katz JL, Wirtz S, Justice JB Jr, and Newman AH (2001) Novel tropane-based irreversible ligands for the dopamine transporter. *J Med Chem* **44:**4453–4461.

Address correspondence to: Roxanne A. Vaughan, Department of Biochemistry and Molecular Biology, University of North Dakota School of Medicine and Health Sciences, Grand Forks, ND 58202. E-mail: rvaughan@medicine.nodak.edu.